J. Am. Chem. Soc. 1982, 104, 7030-7036

Metal Alkoxides: Model for Metal Oxides. 3.[1] Further Studies of the Carbonylation of Hexaalkoxides of Dimolybdenum and Ditungsten ($M\equiv M$) and Characterization of $M_2(O\text{-}i\text{-}Pr)_6(py)_2(\mu\text{-}CO)(M{=}M)$ Compounds

M. H. Chisholm,* J. C. Huffman, J. Leonelli, and I. P. Rothwell

Contribution from the Department of Chemistry and Molecular Structure Center, Indiana University, Bloomington, Indiana 47405. *Received March 25, 1982*

Abstract: Addition of carbon monoxide, 1 atm, 25 °C, to hydrocarbon solutions of $M_2(OR)_6$ ($M\equiv M$) compounds, where M = Mo and W and R = *i*-Pr and Neo (Neo = CH_2CMe_3), in the presence of donor ligands L, leads to the formation of $M_2(OR)_6(L)_2(\mu\text{-}CO)$ compounds, which have been isolated and structurally characterized for R = *i*-Pr and L = pyridine. The molybdenum and tungsten compounds are isomorphous, and in the space group *A*2/*a*, there are four molecules in the unit cell. The cell dimensions for the molybdenum and tungsten compounds are, in that order, a = 18.026 (6), 18.053 (19) Å, b = 18.345 (6), 18.251 (17) Å, and c = 10.569 (3), 10.575 (8) Å with β = 86.74 (1), 87.18 (4)°. The molecules have a crystallographically imposed C_2 axis of symmetry, which contains the carbonyl atoms and bisects the M–M bonds, which have distances of 2.486 (2) and 2.499 (3) Å for M = Mo and W, respectively. The central $M_2O_6N_2C$ skeleton is a confacial bioctahedron with the CO ligand and a pair of O-*i*-Pr groups making up the bridging face. The pyridine ligands are trans to the bridging CO ligand and are weakly held, judging by both the long M–N distances, 2.33 Å (averaged), and the lability of these ligands in solution. The carbonyl C–O distances, 1.21 Å (averaged), are long, comparable to C=O bond distances in ketones. The IR spectra reveal very low ν(CO) values, ca. 1660 cm^{-1} (M = Mo) and 1560 cm^{-1} (M = W). In a formal sense, these compounds have M–M double bonds and may be viewed as inorganic analogues of cyclopropenones. The ^{13}C chemical shifts of the bridging CO ligands (ca. 325 ppm (M = Mo) and 315 ppm (M = W)) occur well downfield from those known for bridging carbonyls in neutral organometallic compounds. The bridging CO moiety may have some bridging oxycarbyne character. In solution, these compounds are fluxional and labile to reversible ligand dissociation on the NMR time scale. They are also reactive toward both loss of CO and reaction with CO, which give $M(CO)_6$ as the principal carbonyl-containing compounds. These findings are discussed in light of previous work and current theories concerning the activation of carbon monoxide.

Introduction

As part of our interest in developing the organometallic chemistry associated with metal alkoxides and in elucidating the possible use of metal alkoxides as hydrocarbon-soluble models[2] for metal oxides, we have continued investigations of the reactions between $M_2(OR)_6$ ($M\equiv M$) compounds (M = Mo, W) and carbon monoxide. Previously, we have shown[3] that these reactions lead to cleavage of the $M\equiv M$ bond and, by disproportionation reactions, to $M(CO)_6$ and alkoxides of higher valent metal species. For $Mo_2(O\text{-}t\text{-}Bu)_6$, we were able to establish that the stoichiometric reaction shown in eq 1 proceeded by an initial reversible reaction leading to the formation of $Mo_2(O\text{-}t\text{-}Bu)_6(\mu\text{-}CO)$.[3]

$$2Mo_2(O\text{-}t\text{-}Bu)_6 + 6CO \rightarrow Mo(CO)_6 + 3Mo(O\text{-}t\text{-}Bu)_4 \qquad (1)$$

The central skeleton of the $Mo_2(O\text{-}t\text{-}Bu)_6(\mu\text{-}CO)$ molecule is shown in I. Each molybdenum atom is in a square-based pyramidal environment. The two metal atoms are joined through a common basal edge formed by a pair of bridging O-*t*-Bu ligands and an apical μ-CO group. From considerations of M–M distance, simple electron counting, and symmetry, we have argued for the existence of a Mo=Mo bond in this molecule. We now show that related compounds of general formula $M_2(OR)_6L_2(\mu\text{-}CO)$ can be isolated for both molybdenum and tungsten when R = *i*-Pr and Neo (Neo = CH_2CMe_3) in the presence of donor ligands. These new compounds show most unusual, if not unprecedented, spectroscopic properties for bridging (μ) carbonyl ligands. In part the unusual aspects of the μ-CO ligand may be rationalized: formally, these compounds are inorganic analogues of cyclopropenones and the bridging carbonyl ligand appears to have some degree of bridging oxycarbyne character as shown in II.

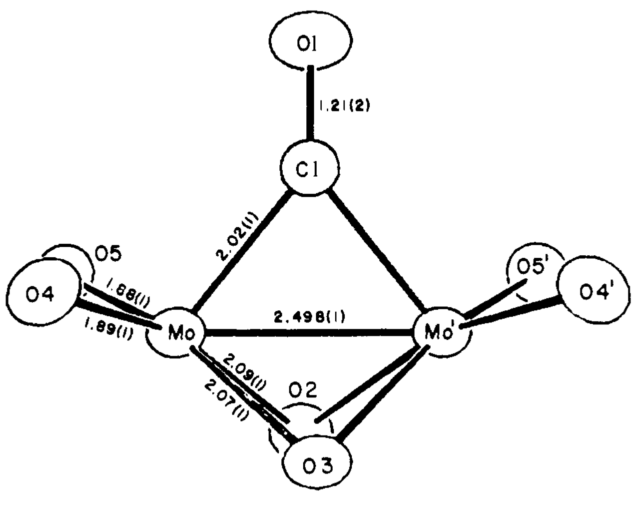

I

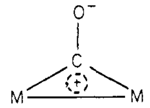

II

Results and Discussion

Synthesis of $M_2(OR)_6L_2(\mu\text{-}CO)$ Compounds. $M_2(OR)_6$ ($M\equiv M$) compounds react reversibly with donor ligands such as pyridine or amines according to eq 2.

$$M_2(OR)_6 + 2L \rightleftharpoons M_2(OR)_6L_2 \qquad (2)$$

The position of equilibrium is dependent on the nature of R, L, and M. For R = *t*-Bu, no simple adducts have been detected; for R = *i*-Pr and L = py, the equilibrium lies to the right for M = W and to the left for M = Mo, though adducts $M_2(O\text{-}i\text{-}$

---

[1] Part 2: Chisholm, M. H.; Folting, K.; Huffman, J. C.; Rothwell, I. P. *J. Am. Chem. Soc.* **1982**, *104*, 4389.

[2] Chisholm, M. H.; Huffman, J. C.; Kirkpatrick, C. C.; Leonelli, J. *J. Am. Chem. Soc.* **1981**, *103*, 6903.

[3] Chisholm, M. H.; Cotton, F. A.; Extine, M. W.; Kelly, R. L. *J. Am. Chem. Soc.* **1979**, *101*, 7645.

0002-7863/82/1504-7030$01.25/0

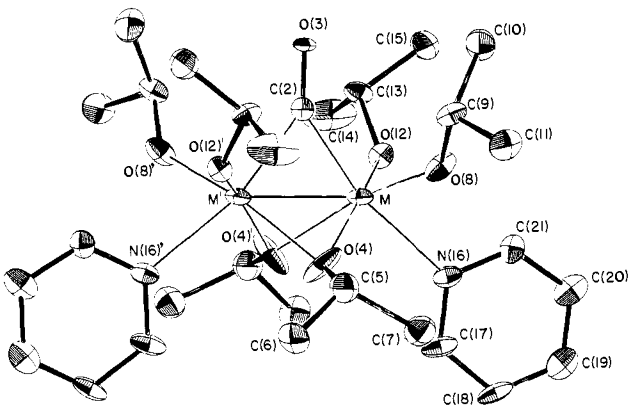

Figure 1. ORTEP view of the $Mo_2(O\text{-}i\text{-}Pr)_6(py)_2(\mu\text{-}CO)$ molecule showing the atom-numbering scheme used in the tables. Primed and unprimed atoms are related by the molecular C_2 axis of symmetry.

$Pr)_6(py)_2$ have been structurally characterized for both metals. For the less sterically demanding neopentoxy ligands, the equilibrium lies to the right for both metals, when L = pyridine and dimethylamine. The solid-state structures of the adducts $Mo_2(OSiMe_3)_6(HNMe_2)_2$[4] and $M_2(O\text{-}i\text{-}Pr)_6(py)_2$, M = Mo,[5] W,[6] reveal four-coordinated metal atoms united by an unbridged M≡M bond. Each MO_3N group is roughly square planar, and the two halves of the molecule are brought together so that the central $M_2O_6N_2$ skeleton is staggered. ^1H NMR studies indicate that in solution this type of structure is preserved.

A common route to the $Mo_2(OR)_6L_2(\mu\text{-}CO)$ compounds involved the addition of 1 atm of CO to the equilibrium mixture (2) in hexane. When the solution was cooled to ca. −15 °C, dark red-purple crystalline compounds $M_2(OR)_6L_2(\mu\text{-}CO)$ were obtained for R = *i*-Pr, L = py, and M = Mo, W and for R = Neo, L = py, $HNMe_2$, and M = Mo, W, in close to 60% yield on the basis of the idealized reaction (3).

$$M_2(OR)_6 + 2L + CO \rightarrow M_2(OR)_6L_2(\mu\text{-}CO) \qquad (3)$$

From the above discussion concerning the equilibrium reaction (2), it is not obvious how the new compounds are formed in (3). They could be formed either by CO attack on the adducts $M_2(OR)_6L_2$ or by initial CO attack on $M_2(OR)_6$ compounds followed by association of L. This question concerning the order of assembly is discussed later.

The new compounds are thermally unstable and do not sublime in vacuo. They readily lose CO and L in the mass spectrometer, yielding $M_2(OR)_6^+$ ions as the ions of highest mass. The pyridine adducts may be stored in sealed vials in vacuo or under a nitrogen atmosphere at room temperature with little or no detectable decomposition. The dimethylamine adducts are, however, less stable in the solid state, and some decomposition is observed upon prolonged storage. In solution, the compounds slowly decompose, though the pyridine adducts are not significantly decomposed for several hours in toluene at room temperature, which allows for their spectroscopic characterization by ^{13}C NMR spectroscopy. Infrared and NMR spectroscopic data for the new compounds are recorded in the Experimental Section.

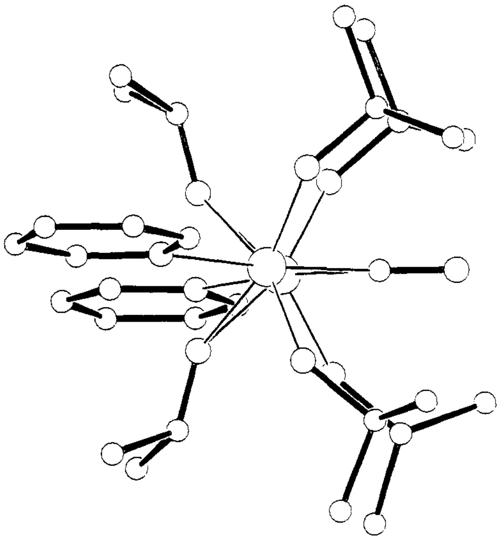

Figure 2. ORTEP view of the $Mo_2(O\text{-}i\text{-}Pr)_6(py)_2(\mu\text{-}CO)$ molecule looking down the Mo–Mo bond, emphasizing the confacial-bioctahedral geometry and the conformations of the isopropyl ligands.

Table I. Fractional Coordinates and Isotropic Thermal Parameters for the $Mo_2(O\text{-}i\text{-}Pr)_6(py)_2(\mu\text{-}CO)$ Molecule[a]

atom	x	y	z	B_{iso}, Å^2
Mo(1)	2335.5 (4)	1591.5 (4)	3874 (1)	14
C(2)	2500[b]	698 (7)	5000[b]	12
O(3)	2500[b]	47 (4)	5000[b]	15
O(4)	1842 (4)	2238 (4)	5326 (6)	41
C(6)	1123 (5)	2910 (5)	6888 (9)	26
C(7)	736 (6)	2825 (5)	4643 (9)	28
O(8)	1405 (3)	1207 (3)	3410 (6)	22
C(9)	931 (5)	627 (5)	3851 (8)	21
C(10)	1102 (5)	−54 (6)	3035 (9)	30
C(11)	127 (5)	873 (5)	3743 (10)	28
O(12)	3004 (3)	1239 (3)	2533 (5)	17
C(13)	3515 (5)	640 (5)	2384 (8)	18
C(14)	4265 (6)	932 (6)	1985 (13)	48
C(15)	3229 (7)	147 (6)	1347 (10)	43
N(16)	2032 (4)	2402 (4)	2292 (7)	18
C(17)	2057 (5)	3120 (5)	2387 (10)	22
C(18)	1835 (5)	3582 (5)	1428 (9)	22
C(19)	1560 (5)	3274 (5)	331 (9)	25
C(20)	1542 (5)	2523 (6)	222 (9)	25
C(21)	1773 (5)	2108 (5)	1242 (8)	19
C(5A)	6191 (11)	2584 (13)	724 (18)	26 (7)
C(5B)	1377 (10)	2844 (12)	5462 (17)	7 (6)

[a] Fractional coordinates are ×10^4 for non-hydrogen atoms. B_{iso} values are ×10. Isotropic values for those atoms refined anisotropically are calculated by using the formula given by: Hamilton, W. C. *Acta Crystallogr.* 1959, *12*, 609. [b] These parameters were not varied.

Solid-State and Molecular Structures of $M_2(O\text{-}i\text{-}Pr)_6(py)_2(\mu\text{-}CO)$, Where M = Mo or W. The molybdenum and tungsten compounds are isomorphous, and in the space group *A*2/*a*, there are four molecules in the unit cell. The molecules have a crystallographic C_2 axis of symmetry bisecting the M–M bond and containing the CO ligand. An ORTEP view of the $Mo_2(O\text{-}i\text{-}Pr)_6(py)_2(\mu\text{-}CO)$ molecule is shown in Figure 1, which also gives the atom-numbering scheme used for both compounds. The methyne carbon atoms of the bridging of O-*i*-Pr ligands are disordered, C(5A) and C(5B), in roughly equal occupancy, but the methyl groups C(6) and C(7) are not. This fact, along with observed conformations of the other isopropyl groups, can be rationallized in terms of the natural tendency to minimize steric repulsive interactions. The carbonyl ligand fits neatly into a pocket or cavity formed by the four methyne groups of the terminal isopropoxy ligands. From simple steric considerations, it would seem impossible to replace the four methyne groups by methyl groups and it is thus not surprising that $M_2(O\text{-}t\text{-}Bu)_6(py)_2(\mu\text{-}CO)$ compounds have not been isolated. In $Mo_2(O\text{-}t\text{-}Bu)_6(\mu\text{-}CO)$, the *tert*-butyl groups are directed below the MoO_4 basal planes, away from the CO ligand, and thus prevent easy access by pyridine.

A view down the Mo-Mo bond is shown in Figure 2. This view emphasizes the confacial bioctahedral geometry of the central $Mo_2O_6CN_2$ skeleton, which leads to the eclipsed conformation for the terminal ligands.

Fractional coordinates and isotropic thermal parameters for the molybdenum and tungsten compounds are given in Tables I

---

(4) Chisholm, M. H.; Cotton, F. A.; Extine, M. W.; Reichert, W. W. *J. Am. Chem. Soc.* **1978**, *100*, 153.

(5) Chisholm, M. H.; Huffman, J. C., results to be submitted for publication.

(6) Akiyama, M.; Chisholm, M. H.; Cotton, F. A.; Extine, M. W.; Haitko, D. A.; Little, D.; Fanwick, P. E. *Inorg. Chem.* **1979**, *18*, 2321.

Table II. Fractional Coordinates and Isotropic Thermal Parameters for the $W_2(O\text{-}i\text{-}Pr)_6(py)_2(\mu\text{-}CO)$ Molecule[a]

atom	x	y	z	B_{iso}, Å^2
W(1)	2330 (1)	1588 (1)	3869 (1)	13
C(2)	2500[b]	699 (18)	5000[b]	10 (7)
O(3)	2500[b]	21 (12)	5000[b]	12 (5)
O(4)	1834 (11)	2253 (11)	5327 (19)	30 (4)
C(6)	1132 (15)	2921 (14)	6898 (24)	16 (5)
C(7)	716 (16)	2834 (16)	4589 (26)	23 (6)
O(8)	1388 (9)	1225 (9)	3384 (15)	15 (3)
C(9)	923 (15)	633 (14)	3843 (24)	17 (5)
C(10)	1109 (15)	9964 (15)	3070 (25)	21 (6)
C(11)	86 (16)	898 (16)	3698 (27)	25 (6)
O(12)	2983 (10)	1251 (9)	2498 (16)	16 (3)
C(13)	3500 (14)	628 (13)	2368 (23)	12 (5)
C(14)	4290 (18)	942 (18)	1988 (30)	35 (7)
C(15)	3212 (17)	153 (17)	1329 (28)	32 (7)
N(16)	2026 (12)	2398 (11)	2275 (20)	14 (4)
C(17)	2067 (16)	3140 (15)	2440 (27)	22 (6)
C(18)	1860 (15)	3607 (13)	1425 (24)	18 (5)
C(19)	1583 (17)	3319 (18)	333 (28)	33 (7)
C(20)	1559 (15)	2556 (14)	227 (25)	17 (5)
C(21)	1776 (15)	2104 (14)	1267 (24)	17 (5)
C(5A)	6191 (32)	2528 (31)	688 (51)	18 (11)
C(5B)	1398 (28)	2916 (27)	5371 (44)	10 (9)

[a] Fractional coordinates are $\times 10^4$ for non-hydrogen atoms. B_{iso} values are $\times 10$. Isotropic values for those atoms refined anisotropically are calculated by using the formula given by: Hamilton, W. C. *Acta Crystallogr.* 1959, *12*, 609. [b] These parameters were not varied.

Table III. Bond Distances for the $M_2(O\text{-}i\text{-}Pr)_6(py)_2(\mu\text{-}CO)$ Molecules

		dist, Å	
A	B	M = Mo	M = W
M(1)	M(1)'	2.486 (2)	2.499 (3)
M(1)	O(4)	2.098 (6)	2.12 (2)
M(1)'	O(4)	2.113 (6)	2.15 (2)
M(1)	O(8)	1.909 (6)	1.91 (2)
M(1)	O(12)	1.920 (5)	1.92 (2)
M(1)	N(16)	2.325 (7)	2.33 (2)
M(1)	C(2)	2.057 (10)	2.06 (3)
O(3)	C(2)	1.194 (13)	1.22 (4)
O(4)	C(5A)	1.266 (19)	1.24 (6)
O(4)	C(5B)	1.395 (20)	1.44 (5)
O(8)	C(9)	1.427 (10)	1.45 (3)
O(12)	C(13)	1.436 (10)	1.47 (3)
N(16)	C(17)	1.323 (11)	1.37 (3)
N(16)	C(21)	1.342 (11)	1.28 (3)
C(6)	C(5A)	1.528 (21)	1.52 (6)
C(6)	C(5B)	1.555 (20)	1.66 (6)
C(7)	C(5A)	1.627 (22)	1.65 (6)
C(7)	C(5B)	1.483 (20)	1.52 (6)
C(9)	C(10)	1.538 (13)	1.50 (3)
C(9)	C(11)	1.529 (13)	1.61 (3)
C(13)	C(14)	1.493 (13)	1.57 (4)
C(13)	C(15)	1.533 (13)	1.51 (3)
C(17)	C(18)	1.397 (13)	1.43 (4)
C(18)	C(19)	1.404 (14)	1.38 (4)
C(19)	C(20)	1.383 (13)	1.42 (4)
C(20)	C(21)	1.402 (13)	1.44 (4)

and II, respectively. Anisotropic thermal parameters are available in the supplementary data. Bond distances and bond angles for the two compounds are given in Tables III and IV, respectively.

The most obvious point to be made from a comparison of the data in Tables III and IV is that the structural parameters are essentially identical for the two compounds, at least within the limits of the experimental error. Furthermore, the M–O bridging and terminal distances and the M–C and carbonyl C–O distances are very similar to those associated with $Mo_2(O\text{-}t\text{-}Bu)_6(\mu\text{-}CO)$, as is shown in I. The M–N distances are long, 2.33 Å (average), which is consistent with the observed ease of pyridine dissociation found in solution (see later). The Mo–N distance of 2.33 Å may be compared with Mo–N = 2.15 Å in $Mo_2(ONeo)_6(\mu\text{-}C_4H_4)(py)$, which is a nonfluxional molecule in solution at room temperature and does not show rapid exchange between free and coordinated pyridine.[1]

Table IV. Bond Angles for the $M_2(O\text{-}i\text{-}Pr)_6(py)_2(\mu\text{-}CO)$ Molecules

			angle, deg	
A	B	C	M = Mo	M = W
M(1)'	M(1)	O(4)	53.5 (2)	53.6 (5)
M(1)'	M(1)	O(8)	120.5 (2)	121.3 (5)
M(1)'	M(1)	O(12)	122.2 (2)	123.1 (5)
M(1)'	M(1)	N(16)	140.1 (2)	140.3 (5)
M(1)'	M(1)	C(2)	52.8 (2)	52.7 (5)
O(4)	M(1)	O(4)'	70.6 (4)	70.5 (12)
O(4)	M(1)	O(8)	93.1 (3)	92.5 (8)
O(4)	M(1)	O(12)'	93.4 (3)	93.6 (8)
O(4)	M(1)	O(12)	161.8 (3)	161.8 (3)
O(4)	M(1)	N(16)	93.3 (3)	93.1 (7)
O(4)	M(1)	C(2)	95.5 (2)	96.0 (7)
O(8)	M(1)	O(12)	102.1 (3)	102.1 (8)
O(8)	M(1)	N(16)	78.8 (2)	77.5 (7)
O(8)	M(1)	C(2)	90.7 (2)	92.3 (6)
O(12)	M(1)	N(16)	81.3 (2)	79.6 (7)
O(12)	M(1)	C(2)	93.1 (2)	94.3 (6)
N(16)	M(1)	C(2)	166.6 (3)	166.7 (7)
M(1)	O(4)	M(1)	72.4 (2)	71.8 (6)
M(1)	O(4)	C(5A)	137.3 (11)	134.7 (30)
M(1)	O(4)	C(5B)	146.9 (9)	148.7 (23)
C(5A)	O(4)	C(5B)	38.8 (10)	38.4 (28)
M(1)	O(8)	C(9)	135.3 (5)	132.3 (14)
M(1)	O(12)	C(13)	135.2 (5)	133.9 (14)
Mo(1)	N(16)	C(17)	124.9 (7)	121.1 (18)
M(1)	N(16)	C(21)	116.4 (6)	115.3 (18)
C(17)	N(16)	C(21)	118.6 (8)	123.5 (25)
M(1)	C(2)	M(1)	74.3 (4)	74.7 (11)
M(1)	C(2)	O(3)	142.8 (2)	142.7 (5)
C(5A)	C(6)	C(5B)	33.7 (9)	32.6 (23)
C(5A)	C(7)	C(5B)	33.0 (9)	32.6 (23)
O(8)	C(9)	C(10)	109.0 (7)	107.9 (21)
O(8)	C(9)	C(11)	107.9 (7)	105.3 (19)
C(10)	C(9)	C(11)	111.0 (8)	112.5 (23)
O(12)	C(13)	C(14)	108.7 (7)	107.9 (20)
O(12)	C(13)	C(15)	106.9 (7)	106.8 (21)
C(14)	C(13)	C(15)	110.2 (9)	112.1 (23)
N(16)	C(17)	C(18)	122.5 (10)	117.5 (26)
C(17)	C(18)	C(19)	118.9 (9)	122.6 (28)
C(18)	C(19)	C(20)	118.7 (9)	115.6 (29)
C(19)	C(20)	C(21)	117.9 (10)	120.2 (26)
N(16)	C(21)	C(20)	123.3 (9)	120.3 (25)
O(4)	C(5A)	C(6)	116.7 (15)	119.5 (42)
O(4)	C(5A)	C(7)	112.4 (15)	115.4 (40)
O(4)	C(5A)	C(5B)	78.4 (20)	83.2 (58)
C(6)	C(5A)	C(7)	105.7 (13)	110.5 (37)
C(6)	C(5A)	C(5B)	74.8 (19)	82.2 (53)
C(7)	C(5A)	C(5B)	64.6 (18)	65.4 (49)
O(4)	C(5B)	C(6)	107.6 (14)	100.4 (33)
O(4)	C(5B)	C(7)	113.9 (14)	111.9 (36)
O(4)	C(5B)	C(5A)	62.8 (18)	58.4 (49)
C(6)	C(5B)	C(7)	111.8 (13)	110.3 (36)

The carbonyl C—O distances in $Mo_2(O\text{-}t\text{-}Bu)_6(\mu\text{-}CO)$ (1.21 (2) Å), $Mo_2(O\text{-}i\text{-}Pr)_6(py)_2(\mu\text{-}CO)$ (1.1944 (13) Å), and $W_2(O\text{-}i\text{-}Pr)_6(py)_2(\mu\text{-}CO)$ (1.22 (4) Å) are comparable to C=O distances of ketones and specifically may be compared with the C—O distances found from microwave studies for cyclopropanone (1.191 (2) Å)[7] and cyclopropenone (1.212 (2) Å).[8]

Infrared and NMR Spectroscopic Studies. Infrared spectra of metal carbonyls have proved to be a rich and convenient source of information concerning both structure and bonding. "For neutral molecules, bridging CO groups (μ-CO) absorb in the range 1700–1860 cm^{-1}."[9] ^{13}C NMR spectra are also often useful, and

---

(7) Pochan, J. M.; Baldwin, J. E.; Flygare, W. H. *J. Am. Chem. Soc.* **1969**, *91*, 1896.

(8) Benson, R. C.; Flygare, W. H.; Oda, M.; Breslow, R. *J. Am. Chem. Soc.* **1973**, *95*, 2772.

(9) Cotton, F. A.; Wilkinson, G. In "Advanced Inorganic Chemistry", 4th ed.; Wiley: New York, 1980.

Table V. Carbonyl Stretching Frequencies, $\bar{\nu}$, for $M_2(OR)_6L_2(\mu\text{-CO})$ Compounds and Some Other Well-Known μ-CO Organometallic Compounds

compd	ν(CO), cm^{-1}	$\nu(^{13}CO)$, cm^{-1}	$\bar{\nu}_{calcd}$-(^{13}CO),[a] cm^{-1}	ref
$Mo_2(O\text{-}i\text{-}Pr)_6(py)_2(\mu\text{-CO})$	1655	1637	1618	*b*
$W_2(O\text{-}i\text{-}Pr)_6(py)_2(\mu\text{-CO})$	1555	1535	1520	*b*
$Mo_2(ONeo)_6(HNMe_2)_2(\mu\text{-CO})$	1660	1630	1623	*b*
$W_2(ONeo)_6(HNMe_2)_2(\mu\text{-CO})$	1570	1542	1535	*b*
$Mo_2(ONeo)_6(py)_2(\mu\text{-CO})$	1660			*b*
$(Cp)_2Fe_2(CO)_2(\mu\text{-CO})_2$	1797 (μ-CO) 1765 (μ-CO)			*c*
$(Cp)_2Ru(CO)_2(\mu\text{-CO})_2$	1764 (μ-CO)			*d*
$Co_2(CO)_8$	1858 (μ-CO)			*e*
$Fe_2(CO)_9$	1828 (μ-CO)			*e*

[a] With the assumption that CO behaves as a single harmonic oscillator: $\bar{\nu}_2 = \bar{\nu}_1(\mu_1/\mu_2)^{1/2}$. [b] This work. [c] Stimson, R. E.; Shriver, D. F. *Inorg. Chem.* 1980, *19*, 1141. [d] Cable, J. W.; Nyholm, R. S.; Sheline, R. K. *J. Am. Chem. Soc.* 1954, *76*, 3373. [e] Sheline, R. K.; Pitzer, K. S. *Ibid.* 1950, *72*, 1107.

Table VI. Comparison of ^{13}C Chemical Shifts of the μ-CO Ligand in $M_2(OR)_6L_2(\mu\text{-CO})$ Compounds with Those of Carbyne Carbon Chemical Shifts

compd	$\delta(^{13}C)$	$J_{^{183}W-^{13}C}$, Hz	solvent	ref
$Mo_2(O\text{-}i\text{-}Pr)_6(py)_2(\mu\text{-CO})$	331.5		C_6D_6	*a*
$W_2(O\text{-}i\text{-}Pr)_6(py)_2(\mu\text{-CO})$	310.4	170 ± 5	C_6D_6	*a*
$Mo_2(ONeo)_6(HNMe_2)_2(\mu\text{-CO})$	324		C_6D_6	*a*
$W_2(ONeo)_6(HNMe_2)_2(\mu\text{-CO})$	319.6	160 ± 5	C_6D_6	*a*
$Mo_2(ONeo)_6(py)_2(\mu\text{-CO})$	323.6		C_6D_6	*a*
$W_2(\mu\text{-CSiMe}_3)_2(CH_2SiMe_3)_4$	352.6		C_7D_8	*b*
$W(CCMe_3)(CH_2CMe_3)_3$	324	230 ± 5	C_6D_6	*c*
$(Cp)_3Rh_3(\mu_3\text{-CO})(\mu_3\text{-CH})$	210.5 (CO) 303.6 (CH)		DMF-d_7	*d*

[a] This work. [b] Chisholm, M. H.; Cotton, F. A.; Extine, M. W.; Stults, B. R. *Inorg. Chem.* 1976, *15*, 2252. [c] Clark, D. N.; Schrock, R. R. *J. Am. Chem. Soc.* 1978, *100*, 6774. [d] Herrmann, W. A.; Plank, J.; Riedel, D.; Ziegler, M. L.; Weidenhammer, K.; Guggolz, E.; Balbach, B. *Ibid.* 1981, *103*, 63.

bridging carbonyls are generally found in the range 220–240 ppm downfield from Me_4Si,[10] which is at lower field than terminal CO groups. In both of these regards, the new carbonyl compounds reported herein show anomalous spectroscopic properties. The low ν(CO) values, ca. 1660 cm^{-1} for M = Mo and 1560 cm^{-1} for M = W, and the chemical shift values, ca. 325 ppm for M = Mo and 315 ppm for M = W, are unprecedentedly low when compared to all known organometallic compounds having a μ-CO group (see Tables V and VI).

The fact that for related alkoxy compounds alkoxy compounds ν(CO) is roughly 100 cm^{-1} lower for tungsten than for molybdenum is particularly fascinating. Since the formal oxidation state of the metal atoms is +3, this observation may be correlated with the fact that the effective charge exerted on the valence electrons is less for W than for Mo because W has 32 more electrons. Thus, for related compounds in oxidation state +3, tungsten should be a better π donor to π^*-acceptor ligands such as CO. This line of reasoning has been used to account for the changes in ν(NO) for a related series of compounds of formula $M_2(OR)_6(NO)_2$, which are ca. 1720 (Cr), 1640 (Mo), and 1560 cm^{-1} (W).[11] One must, of course, identify what number of metal d electrons are available for back-bonding to the CO ligand and furthermore inspect the symmetry constraints of the molecule. To do this, we should recognize that each metal atom is in an octahedral environment, and with the bridging CO ligand counted as donating one electron to each metal, there are two electrons per metal in t_{2g}-type orbitals that are not used in forming metal–ligand σ bonds. Collectively, these four electrons could be used to form a metal–metal double bond, $\sigma^2\pi^2$, or a metal–metal single bond and a metal–carbon double bond as shown in the resonance forms III–V.

Scheme I. Proposed Reaction Pathway for the Formation of $M_2(OR)_6(py)_2(\mu\text{-X})$ Compounds; M = Mo, W; X = Co, HCCH

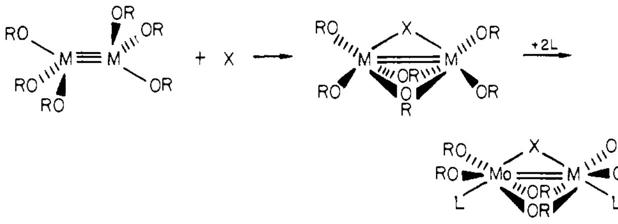

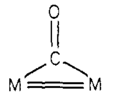

III

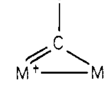

IV

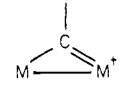

V

An analogy with cyclopropenone is thus apparent, and extensive mixing of M–M and C–O bonding is evident. Finally, it should be noted that the presence of terminal RO ligands, which are capable of π donating to metal t_{2g} orbitals, could further enhance back-bonding from metal-to-CO π^* orbitals.[12] All of these factors contribute to the oxycarbyne character, II, of the bridging carbonyl ligand. Finally, the low-field ^{13}C shifts and the magnitude of ${}^1J_{^{183}W-^{13}C}$ for the carbonyl group may also be reconsidered with a bridging carbyne ligand, for which shifts generally occur below 300 ppm (see Table VI).

Dynamical Solution Behavior. At room temperature in toluene-d_8, ^1H NMR spectra indicate rapid exchange of terminal and bridging alkoxy groups. Furthermore, there is evidently rapid exchange between free and coordinated pyridine. Upon a lowering of the temperature, the initially sharp resonances broaden, then collapse, and finally, below −40 °C at 220 MHz, give rise to a low-temperature limiting spectrum that is consistent with the structure found in the solid state. Specifically, the ^1H NMR spectra show two types of OR ligands in the ratio 2:1 and the methylene protons of the O(Neo) terminal groups and the methyl groups of the O-*i*-Pr terminal ligands are diastereotopic. Exchange between free and coordinated pyridine is frozen out. All of these observations are independent of the concentration of added pyridine in the range of 1–10 equiv. The same type of behavior was observed for the bridging acetylene complexes $Mo_2(OR)_6(py)_2(\mu\text{-}C_2R'_2)$, where R = *i*-Pr, R′ = H and R = Neo, R′ = H, Me. A common reaction pathway is thus indicated for these compounds of formula $M_2(OR)_6(\mu\text{-X})(L)_2$ involving initial dissociation of L. This leads to stereochemically nonrigid $Mo_2(OR)_6(\mu\text{-X})$ compounds that are labile toward release of X (X = CO or R′CCR′) with regeneration of the triply bonded and unbridged compounds $M_2(OR)_6$. By the law of microscopic reversibility, we thus propose the reaction sequence shown in Scheme I for the assembly of these $M_2(OR)_6(L)_2(\mu\text{-X})$ compounds.

Direct evidence for the lability of the CO ligand in these compounds is seen in the following reactions. When Mo_2-

---

(10) Chisholm, M. H.; Godleski, S. *Prog. Inorg. Chem.* **1970**, *20*, 299.

(11) Bradley, D. C.; Newing, C. W.; Chisholm, M. H.; Kelly, R. L.; Haitko, D. A.; Little, D.; Cotton, F. A.; Fanwick, P. E. *Inorg. Chem.* **1980**, *19*, 3010.

(12) The π-donor influence of RO ligands on π^*-acceptor ligands bonded to Mo(2+) has been seen in the unusual properties of the compounds $Mo(O\text{-}t\text{-}Bu)_2(py)_2(CO)_2$ and $Mo(O\text{-}i\text{-}Pr)_2(bpy)_2$. See: Chisholm, M. H.; Huffman, J. C.; Kelly, R. L. *J. Am. Chem. Soc.* **1979**, *101*, 7615. Chisholm, M. H.; Huffman, J. C.; Rothwell, I. P.; Bradley, P. G.; Kress, N.; Woodruff, W. H. *Ibid.* **1981**, *103*, 4945.

$(ONeo)_6(py)_2(^{13}CO)$ and $Mo_2(O\text{-}i\text{-}Pr)_6$ were mixed in roughly equimolar quantities and dissolved in toluene-d_8, the ^{13}C NMR spectrum recorded within 1 h showed the formation of $Mo_2(O\text{-}i\text{-}Pr)_6(py)_2(^{13}CO)$. $Mo_2(O\text{-}i\text{-}Pr)_6(py)_2(^{13}CO)$ was also the predominant species present when 1 equiv of ^{13}CO was added to an equimolar mixture of $Mo_2(O\text{-}i\text{-}Pr)_6$ and $Mo_2(ONeo)_6(py)_2$ dissolved in toluene-d_8. Finally, when they are heated in vacuo, all these compounds lose CO and pyridine: only $Mo_2(OR)_6$ compounds sublime. The order of lability of the ligands in $M_2(OR)_6(py)_2(\mu\text{-}CO)$ compounds is reversible py dissociation > bridge–terminal OR exchange > reversible CO dissociation.

Why is it that reversible carbonyl addition across the M≡M bond is such a facile process? We believe the answer to this question lies in the fact that the $M_2(OR)_6$ compounds are coordinatively unsaturated and attack by CO as a Lewis base at one metal provides an easy point of attack and departure. The linear cheleotropic reaction,[13] eq 4, is no more favored for the metal–metal triple bond than it is for the carbon–carbon triple bond.

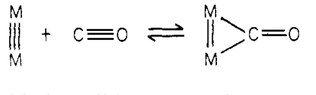

(4)

Carbon monoxide is well known to cleave metal–metal single bonds, but these reactions generally require high temperatures and pressures.[14] By contrast, reversible CO addition to $Os_3(\mu\text{-}H)_2(CO)_{10}$, which contains an Os=Os bond, and reversible cleavage of the Pd–Pd bond in eq 5[15] occur with great ease.

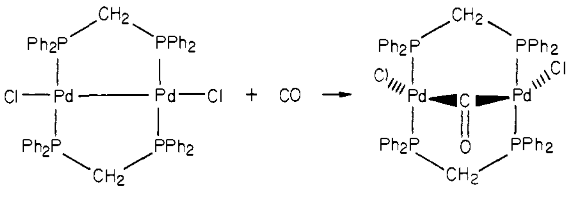

(5)

The key feature to these facile reversible carbonyl addition reactions involves the presence and stability of coordinatively unsaturated metal centers.

Pathway to Cleavage of the M≡M Bond. The facile cleavage of the M≡M bond, which occurs at 25 °C and 1 atm CO in eq 1 and is observed for alkoxides other than the *tert*-butoxide, is quite remarkable. A general reaction scheme leading to this cleavage can be based upon the formation of $M_2(OR)_6(\mu\text{-}CO)$ intermediates akin to that characterized for M = Mo and R = *t*-Bu. In the presence of pyridine, or other donor ligands, $M_2(OR)_6L_2(\mu\text{-}CO)$ compounds can be isolated for less sterically demanding R groups such as *i*-Pr and Ne. The stabilizing influence of L is twofold. When L is bound, CO is not released and further CO attack on the dimetal complex is blocked. The fact that the ligands L readily dissociate means that cleavage of the M≡M bond is kinetically surpressed but not stopped in solution. ^{13}C NMR spectra of $M_2(OR)_6L_2(\mu\text{-}^{13}CO)$ compounds always show the presence of $M(CO)_6$ compounds, which increase in concentration with time.

When ^{13}CO is added to a benzene-d_6 solution of $Mo_2(O\text{-}i\text{-}Pr)_6$, a transient ^{13}C signal is seen at $\delta = 278.8$ along with a signal at $\delta = 201$, $Mo(CO)_6$, which increases with time. The former signal can reasonably be assigned to $Mo_2(O\text{-}i\text{-}Pr)_6(\mu\text{-}CO)$, cf. $\delta = 272.5$ found for μ-CO in $Mo_2(O\text{-}t\text{-}Bu)_6(\mu\text{-}CO)$.[3]

When ^{13}CO was added to $Mo_2(O\text{-}i\text{-}Pr)_6$ dissolved in benzene-d_6/*i*-PrOH (50:50 by volume), the ^{13}C NMR spectrum showed signals at 319.6 and 278.8 ppm along with a signal at 201 ppm assignable to $Mo(CO)_6$. The formation of $Mo(CO)_6$ was suppressed in this case relative to the reaction carried out in pure benzene-d_6. It is possible that the signals at $\delta = 319.6$ and 278.8 result from $Mo_2(O\text{-}i\text{-}Pr)_6(HO\text{-}i\text{-}Pr)_2(\mu\text{-}CO)$ and $Mo_2(O\text{-}i\text{-}Pr)_6(\mu\text{-}CO)$, respectively, but this remains uncertain.

If it is accepted that donor ligands in $M_2(OR)_6L_2(\mu\text{-}CO)$ compounds block further reaction with CO, then the next step leading toward M–M bond rupture can be viewed as CO attack on $M_2(OR)_6(\mu\text{-}CO)$ or $M_2(OR)_6L(\mu\text{-}CO)$ compounds. Some support for this is seen in the following.

The IR spectrum of a Nujol mull (solution) of $Mo_2(ONeo)_6(HNMe_2)_2(\mu\text{-}CO)$ shows initially a strong band at 1660 cm^{-1} assignable to $\nu(CO)$ in this compound. With time, however, two new bands appear at 1691 (broad) and 1940 cm^{-1}, followed by absorption at 1988 cm^{-1} assignable to $Mo(CO)_6$. It is not unreasonable to assign the bands at 1691 and 1940 cm^{-1} to bridging and terminal CO ligands, respectively, of a species of formula $Mo_2(ONeo)_6(HNMe_2)(CO)_2$ or $Mo_2(ONeo)_6(CO)_2$, whose structure could be closely related to that of $Mo_2(O\text{-}t\text{-}Bu)_6(\mu\text{-}CO)$ and $M_2(O\text{-}i\text{-}Pr)_6(py)_2(\mu\text{-}CO)$ compounds. Subsequent disproportionation to $Mo(OR)_4$ and "$Mo(OR)_2(CO)_2$" could occur. The latter species may be trapped by pyridine, as in the isolation of $Mo(O\text{-}t\text{-}Bu)_2(py)_2(CO)_2$, or may react further via CO and OR group transfer leading ultimately to the formation of $Mo(CO)_6$, which occurs so readily in the absence of donor ligands. While this suggestion is open to conjecture, it does offer a reasonable explanation for the observed facile cleavage of the M≡M bonds in $M_2(OR)_6$ compounds by CO under such mild conditions. Evidence for the formation of the reactive species $Mo_2(O\text{-}i\text{-}Pr)_6(\mu\text{-}CO)$ is seen in the transient appearance of a $\nu(CO)$ band at 1689 cm^{-1} and a ^{13}C resonance at 278.8 ppm when CO is added to hydrocarbon solutions of $Mo_2(O\text{-}i\text{-}Pr)_6$. The formation of $Mo(CO)_6$ is suppressed by even weakly donating ligands such as isopropyl alcohol: When CO (1 atm) is exposed to $Mo_2(O\text{-}i\text{-}Pr)_6$ in benzene-d_6 and *i*-PrOH (ca. 50:50), two resonances, one at 319.6 and the other at 278.8 ppm, are observed in addition to a signal assignable to $Mo(CO)_6$, which grows only slowly with time. It is tempting to assign the downfield signal (319.6 ppm) to the species $Mo_2(O\text{-}i\text{-}Pr)_6(i\text{-}PrOH)_2(\mu\text{-}CO)$ and the higher field signal to the unsolvated species.

The exceedingly low values of $\nu(CO)$ in these compounds suggest that the carbonyl oxygen may be quite basic. Bridging carbonyls are known to act as donors to Lewis acids such as boron and aluminum halides and aluminum alkyls.[16,17] They may also, in some cases, be protonated or alkylated.[18,19] Does the μ-CO group in these new compounds have Lewis base properties? This question will be addressed in future work, and we only note here in passing that solutions of $Mo_2(O\text{-}i\text{-}Pr)_6$ and $Ti(O\text{-}i\text{-}Pr)_4$ readily react with CO. Through the agency of O bridges $Ti(O\text{-}i\text{-}Pr)_4$ may serve as both a Lewis acid and a Lewis base. It is possible here to envisage the formation of linkages of the type shown in VI.

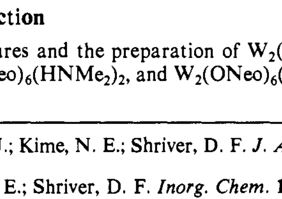

VI

Further studies are planned.

Experimental Section

General procedures and the preparation of $W_2(O\text{-}i\text{-}Pr)_6(py)_2$, $Mo_2(O\text{-}i\text{-}Pr)_6$, $Mo_2(ONeo)_6(HNMe_2)_2$, and $W_2(ONeo)_6(HNMe_2)_2$ have been

---

[13] Woodward, R. B.; Hoffmann, R. "The Conservation of Orbital Symmetry"; Academic Press: New York, 1970; p 152.

[14] Chisholm, M. H.; Rothwell, I. P. *Prog. Inorg. Chem.* **1982**, *29*, 32.

[15] Colton, R.; McCormick, M. J.; Pannan, C. D. *J. Chem. Soc., Chem. Commun.* **1977**, 823. $Pd_2(dam)_2Cl_2(\mu\text{-}CO)$ shows $\nu(CO)$ at 1720 cm^{-1}.

[16] Nelson, N. J.; Kime, N. E.; Shriver, D. F. *J. Am. Chem. Soc.* **1969**, *91*, 5173.

[17] Stimson, R. E.; Shriver, D. F. *Inorg. Chem.* **1980**, *19*, 1141.

[18] Whitmire, K. H.; Shriver, D. F. *J. Am. Chem. Soc.* **1981**, *103*, 6754.

[19] The low-field chemical shifts reported in this paper may be compared to the low values reported for compounds containing η^2-CO and η^2-COH groups; e.g., $\delta = 281$ for η^2-CO in $[PPN][HFe_4(CO)_{13}]$ and $\delta = 294$ for η^2-COH in $HFe_4(CO)_{12}(\eta\text{-}COH)$ (see ref 18 and references therein). The η^2-CO and η^2-COH ligands can also be viewed as bridging oxy- and hydroxycarbyne ligands.

described previously.[6,20] Dry and oxygen-free solvents were used at all times.

^{1}H and ^{13}C NMR spectra were recorded on Varian HA220, XL100, and HX270 spectrometers. Infrared spectra were obtained from Nujol mulls between CsI plates with a Perkin-Elmer 273 spectrometer. ^{13}CO (99% ^{13}C) was obtained from Monsanto Research Corp., Miamisburg, OH. Mass spectra were obtained by the method of direct insertion using an AE1 MS902 spectrometer.[4] Elemental analyses were obtained from the Canadian Microanalytical Service Ltd., Vancouver, B. C., and from Alfred Bernhard, Elbach, West Germany, but data were not satifactory.

Preparation of $W_2(O\text{-}i\text{-}Pr)_6(py)_2(\mu\text{-}CO)$. $W_2(O\text{-}i\text{-}Pr)_6(py)_2$ (330 mg, 0.375 mmol) was dissolved in a hexane/pyridine (15/0.5 mL) solution and exposed to CO (1 atm) at 0 °C with use of gas line techniques. The mixture was cooled to −15 °C in a freezer. After 1 h, red-brown crystals of $W_2(O\text{-}i\text{-}Pr)_6(py)_2(\mu\text{-}CO)$ (200 mg, 59% yield based on W) were obtained and dried in vacuo.

Infrared data in the range 1700–200 cm^{-1}: 1601 s, sh, 1555 s, sh, (^{13}CO, 1535 s, sh), 1480 m, sh, 1460 s, sh, 1445 s, sh, 1400 m, sh, 1372 s, sh, 1360 s, sh, 1325 s, sh, 1255 m, sh, 1212 m, sh, 1160 s, sh, 1110 s, br, 1020 m, sh, 1030 s, sh, 970 s, br, 940 s, sh, 870 s, 840 s, sh, 810 s, br, 690 s, sh, 590 s, sh, 450 m, br, 310 m, sh, 295 m, sh (sh = shoulder).

^{1}H NMR data obtained at 220 MHz, +16 °C, from a toluene-d_8 solution: δ(py α(CH)) 8.95, δ(py γ(CH)) 7.02, δ(py β(CH)) 6.75, δ(OCHMe$_2$) 5.11 (J_{HH} = 6 Hz), δ(OCHMe_2) 1.35 (J_{HH} = 6 Hz) (δ downfield of Me$_4$Si).

^{13}C NMR data obtained at 25.2 MHz, +34 °C, from a benzene-d_6 solution: $\delta(W_2(\mu\text{-}^{13}CO))$ 310.4 ($J_{^{183}WC}$ = 170 Hz), δ(py (CH)) 150.3, δ(py (CH)) 135.8, δ(py (CH)) 123.5, δ(CH) 76.4, δ(CH$_3$) 27.4 (δ downfield of Me$_4$Si).

Anal. Calcd for $W_2O_7C_{29}H_{52}N_2$: C, 38.34; H, 5.73; N, 3.08. Found: C, 36.41; H, 5.22; N, 3.31.

Preparation of $Mo_2(O\text{-}i\text{-}Pr)_6(py)_2(\mu\text{-}CO)$. $Mo_2(O\text{-}i\text{-}Pr)_6$ (850 mg, 1.557 mmol) was dissolved in a hexane/pyridine (25/0.7 mL) solution and exposed to CO (1 atm). The resulting red solution was placed in a freezer at −15 °C for 0.5 h. Deep red crystals of $Mo_2(O\text{-}i\text{-}Pr)_6(py)_2(\mu\text{-}CO)$ (710 mg, 62% based on Mo) were filtered and dried in vacuo.

IR data in the range 1700–200 cm^{-1}: 1655 s, (^{13}CO, 1637 s), 1601 m, 1483 m, 1325 m, 1310 w, 1260 m, 1217 m, 1160 m, 1150 m, 1115 vs, 1070 m, 1040 m, 1012 m, 970 s, 840 ms, 780 mw, 750 m, 698 ms, 616 mw, 600 s, 530 w, 450 mw, 320 m.

^{1}H NMR data obtained at 220 MHz, −40 °C, from a toluene-d_8 solution: δ(py α(CH)) 9.10, δ(py γ(CH)) 6.95, δ(terminal OCHMe$_2$) 5.19 (J_{HH} = 6 Hz), δ(bridge OCHMe$_2$) 3.60 (J_{HH} = 6 Hz), δ(terminal OCHMe_2) 1.81, 1.21 (J_{HH} = 6 Hz), δ(bridge OCHMe_2) 0.87 (J_{HH} = 6 Hz) (δ downfield from Me$_4$Si).

^{13}C NMR data obtained at 67.89 MHz, +25 °C, from a benzene-d_6 solution: $\delta(Mo_2(\mu\text{-}^{13}CO))$ 331.5, δ(py (CH)) 150.3, δ(py (CH)) 135.3, δ(py (CH)) 123.4 (δ downfield from Me$_4$Si).

Satisfactory analysis could not be obtained.

Preparation of $W_2(ONeo)_6(HNMe_2)_2(\mu\text{-}CO)$. $W_2(ONeo)_6(HNMe_2)_2$ (182 mg, 0.186 mmol) was dissolved in hexane (10 mL) and exposed to CO (1 atm) at 0 °C. The mixture was cooled in a freezer at −15 °C for 1 h. Golden brown crystals of $W_2(ONeo)_6(HNMe_2)(\mu\text{-}CO)$ (130 mg, 70% yield based on W) were obtained and dried in vacuo.

IR data in the range 1700–200 cm^{-1}: 1570 s, sh, (^{13}CO, 1542 s, sh), 1465 s, sh, 1395 m, sh, 1380 s, sh, 1365 s, sh, 1260 m, 1220 m, 1060 s, br, 1020 vs, sh, 985 m, 900 s, sh, 800 w, br, 755 m, sh, 720 w, 660 s, sh.

^{1}H NMR data obtained at 220 MHz, +16 °C, from benzene-d_6 solution: δ(terminal OCH_2CMe$_3$) 4.60, δ(bridge OCH_2CMe$_3$) 4.49, δ(HNMe_2) 2.26, δ(terminal OCH$_2$CMe_3) 1.01, δ(bridge OCH$_2$CMe_3) 0.99 (δ downfield from Me$_4$Si).

^{13}C NMR data obtained at 67.89 MHz, +34 °C, from benzene-d_6 solution: $\delta(W_2(\mu\text{-}^{13}CO))$ 319.6 ($J_{^{183}W^{13}C}$ = 160 Hz), δ(OCH$_2$CMe$_3$) 87.0, δ(OCH$_2$$CMe_3$) 34.8, δ(OCH$_2$CMe_3) 27.4 (δ downfield from Me$_4$Si).

Preparation of $Mo_2(ONeo)_6(HNMe_2)_2(\mu\text{-}CO)$. $Mo_2(ONeo)_6(HNMe_2)_2$ (500 mg, 0.623 mmol) was dissolved in hexane (10 mL) and exposed to CO (1 atm). The resulting red solution was cooled to −15 °C in a freezer for 0.5 h. Deep red crystals of $Mo_2(ONeo)_6(HNMe_2)(\mu\text{-}CO)$ (300 mg, 58% yield based on Mo) were filtered and dried in vacuo.

IR data in the range 1700–200 cm^{-1}: 1660 s (^{13}CO, 1630 s), 1480 mw, 1360 m, 1260 mw, 1215 m, 1145 mw, 1050 vs, 1020 s, 800 mw, 755 m, 700 ms, 660 s, 454 s, 454 m, 404 mw, 340 w.

^{1}H NMR data obtained at 220 MHz, +16 °C, from toluene-d_8 solution: δ(terminal OCH_2CMe$_3$) 4.80, 3.79 ($J_{H_AH_B}$ = 12 Hz), δ(bridge CH_2CMe$_3$) 3.48, δ(HNMe_2) 2.54, δ(terminal OCH$_2$CMe_3) 1.17, δ(bridge OCH$_2$CMe_3) 0.82 (δ downfield from Me$_4$Si).

^{13}C NMR data obtained at 67.89 MHz, +20 °C, from a benzene-d_6 solution: $\delta(Mo_2(\mu\text{-}^{13}CO))$ 324.0 (δ downfield from Me$_4$Si).

Satisfactory analysis could not be obtained.

Preparation of $Mo_2(ONeo)_6(py)_2(\mu\text{-}CO)$. $Mo_2(ONeo)_6(py)_2$ (500 mg, 0.594 mol) was dissolved in hexane/pyridine (15/0.5 mL) solution and was exposed to CO (1 atm). The resulting red solution was cooled in a freezer at −15 °C for 0.5 h. Deep red crystals of $Mo_2(ONeo)_6(py)_2(\mu\text{-}CO)$ (350 mg, 67% yield based on Mo) were filtered and dried in vacuo.

IR data in the range 1700–200 cm^{-1}: 1660 s, 1600 m, 1480 mw, 1360 m, 1260 mw, 1215 m, 1145 mw, 1050 vs, 1020 s, 800 mw, 755 m, 700 ms, 660 s, 454 m, 404 m, 340 w.

^{1}H NMR data obtained at 220 MHz, +16 °C, from a benzene-d_6 solution: δ(py α(CH)) 9.10, δ(py γ(CH)) 6.96, δ(py β(CH)) 6.85, δ(OCH_2CMe$_3$) 4.20, δ(OCH$_2$CMe_3) 1.01 (δ downfield from Me$_4$Si).

^{13}C NMR data obtained at 67.89 MHz, +20 °C, from a benzene-d_6 solution: $\delta(Mo_2(\mu\text{-}^{13}CO))$ 323.6 (δ downfield from Me$_4$Si).

$Mo_2(O\text{-}i\text{-}Pr)_6$ + CO. In a 5-mm NMR tube, $Mo_2(O\text{-}i\text{-}Pr)_6$ (ca. 30 mg) was dissolved in benzene-d_6 (ca. 0.5 mL). The NMR tube was sealed under ca. 1 atm ^{13}CO; the solution turned red immediately upon exposure to CO. The NMR tube was placed in the probe of a ^{13}C NMR spectrometer, and data were collected each 60 min for a period of 10 h. The first spectrum showed the formation of resonances at δ = 278.8 and 201. With each successive hour, the resonance at 201 ppm grew at the expense of that at 278.8 ppm. These resonances are assigned to $Mo_2(O\text{-}i\text{-}Pr)_6(\mu\text{-}CO)$ (278.8 ppm) and $Mo(CO)_6$ (201 ppm). When a Nujol solution of $Mo_2(O\text{-}i\text{-}Pr)_6$ was exposed to a CO atmosphere, the solution turned red and showed in the infrared spectrum a band at 1689 cm^{-1}, which we assign to $Mo_2(O\text{-}i\text{-}Pr)_6(\mu\text{-}CO)$.

$Mo_2(O\text{-}i\text{-}Pr)_6$ + HO-i-Pr + ^{13}CO. When a solution of $Mo_2(O\text{-}i\text{-}Pr)_6$ (ca. 30 mg) in benzene/i-PrOH (1 mL 50:50) in a 5-mm NMR tube was exposed to 1 atm ^{13}CO, the solution turned red. The tube was sealed and placed in the probe of an NMR spectrometer. Data were collected every 60 min for a 6-h period. The first spectrum showed resonances at 319.6, 298.8, and 201 ppm. With time, the resonance at 201 ppm assignable to $Mo(CO)_6$ grew at the expense of the others. The resonances at 319.6 and 298.8 ppm are in the region expected for $Mo_2(O\text{-}i\text{-}Pr)_6L_2(\mu\text{-}CO)$ and $Mo_2(O\text{-}i\text{-}Pr)_6(\mu\text{-}CO)$ compounds, L = i-PrOH.

$Mo_2(O\text{-}i\text{-}Pr)_6$ + $Ti(O\text{-}i\text{-}Pr)_4$ + ^{13}CO. To a solution of $Mo_2(O\text{-}i\text{-}Pr)_6$ (ca. 100 mg) in benzene-d_6 (2 mL) was added $Ti(O\text{-}i\text{-}Pr)_4$ (1 mL). This solution was exposed to 1 atm ^{13}CO; the solution turned red. A portion of the sample was placed in an NMR tube, and data were collected each 60 min for a period of 9 h. The initial spectrum showed along with the formation of some $Mo(CO)_6$, δ = 201 ppm, resonances at 294 and 284 ppm, which could be assigned to $Mo_2(O\text{-}i\text{-}Pr)_6(\mu\text{-}CO)(Ti(O\text{-}i\text{-}Pr)_4)_n$-containing species. With time, the signal at 294 ppm decreased and the signals at 201 ($Mo(CO)_6$) and 284 ppm grew. After 6 h, the signal at 284 ppm lost intensity compared to that for $Mo(CO)_6$ at 201 ppm.

X-ray Structural Determinations. General procedures were as described previously.[17]

$Mo_2(O\text{-}i\text{-}Pr)_6(py)_2(\mu\text{-}CO)$. A red crystal of dimensions 0.16 × 0.13 × 0.19 mm was selected and transferred to the cold stream of the goniostat under an atmosphere of dry nitrogen. The cell dimensions obtained from 28 reflections at −166 °C with Mo Kα (λ = 0.71069 Å) were a = 18.026 (6) Å, b = 18.345 (6) Å, c = 10.569 (3) Å, β = 86.74 (1)°, V = 3489 (1) Å^3, Z = 4, and d_{calcd} = 1.395 g cm^{-3} with space group $A2/a$.

A total number of 3601 reflections was collected with use of standard moving-crystal moving-detector techniques with the following values: scan speed 4° min^{-1}, scan width 2.0 + dispersion, single background at extremes of scan 4 s, aperture size 3.0 × 4.0 mm. The limits of data collection were $5° < 2\theta < 50°$. Of the 3601 reflections collected, the number of unique reflections was 2299 and the number with $F > 2.33\sigma(F)$ was 1837. The linear absorption coefficient was 7.414 cm^{-1}.

The structure was solved by a combination of direct methods and Fourier techniques. During refinement, it was found that one of the carbon atoms of the bridging isopropoxy groups was disordered. The two positions (C(5A) and C(5B)) were included in the final refinements, and a population parameter was included. All atoms with the exception of those involved in the disorder were assigned anisotropic thermal parameters. Final occupancy parameters for C(5A) and C(5B) were 0.45 (5) and 0.58 (5), respectively. A final difference Fourier synthesis was essentially featureless, the largest peak being 0.88 e Å^{-3}. While many of the top peaks were located in positions corresponding to the expected hydrogen locations, no attempt was made to include them in the refinement. The final residuals are $R(F)$ = 0.053 and $R_w(F)$ = 0.056. The goodness of fit for the last cycle was 1.382 and the maximum Δ/σ was 0.05.

$W_2(O\text{-}i\text{-}Pr)_6(py)_2(\mu\text{-}CO)$. Samples of $W_2(O\text{-}i\text{-}Pr)_6(py)_2(\mu\text{-}CO)$ generally consisted of irregular crystalline blocks that could be cleaved only with difficulty. Several attempts to obtain good crystals were unsuc-

---

(20) Chisholm, M. H.; Cotton, F. A.; Murillo, C. A.; Reichert, W. W. *Inorg. Chem.* **1977**, *16*, 1801.

(21) Huffman, J. C.; Lewis, L. N.; Caulton, K. G. *Inorg. Chem.* **1980**, *19*, 2755.

cessful, so a sample of questionable quality for X-ray studies was finally used. The crystal studied was cleaved from a larger one in a nitrogen-filled glovebag and transferred under a nitrogen atmosphere to the cold stream of the goniostat. After the crystal was cooled to −161 °C, a search of a limited hemisphere of reciprocal space located reflections that were indexable as monoclinic, space group *A*2/*a*. The structure was in fact isomorphous with the molybdenum analogue, and the cell was chosen to agree with the latter. The cell dimensions obtained at −161 °C from 54 reflections with Mo Kα (λ = 0.710 69 Å) were a = 18.053 (19) Å, b = 18.251 (17) Å, c = 10.575 (8) Å, β = 87.18 (4)°, V = 3480 (2) Å, Z = 4, and d_{calcd} = 1.734 g cm^{-3} with space group *A*2/*a*.

A total number of 3494 reflections was collected with use of standard moving-crystal moving-detector techniques with the following values: scan speed 4.0° min^{-1}, scan width 2.0 + dispersion, single background time at extremes of scan 5 s, aperture size 3.0 × 4.0 mm. The limits of data collection were $5° < 2\theta < 50°$. Of the 3494 reflections collected, 2294 reflections were unique. The number of reflections with $F > 2.33\sigma(F)$ was 1627.

The fractional coordinate for $Mo_2(O\text{-}i\text{-}Pr)_6(py)_2(\mu\text{-}CO)$ were used as a starting point for the refinement. As in the case of the molybdenum compound, a disorder was apparent in the bridging isopropoxy groups. Isotropic refinement converged to $R(F)$ = 0.123 and $R_w(F)$ = 0.109. While the faces of the crystal were uneven, due to fracturing, approximate indices could be assigned. With use of these indices and the crystal dimensions, an analytical absorption correction was performed (μ(Mo Kα) = 67.89 cm^{-1}, maximum and minimum absorption 0.61 and 0.95).

The final residuals are $R(F)$ = 0.0769 and $R_w(F)$ = 0.0584, and the maximum Δ/σ for the last cycle was 0.05 for the absorption-corrected data. When attempts were made to assign anisotropic thermal parameters to the light atoms of the structure, the residual did not indicate a significant improvement.

A final difference Fourier synthesis contained several peaks of intensity 1.3–2.4 e Å^{-3} within 1 Å of the tungsten atoms but otherwise was featureless. The rather poor precision of the structure is undoubtedly due to a combination of the disorder and a poor absorption correction.

Acknowledgment. We thank the Office of Basic Sciences, Chemistry Division, U.S. Department of Energy, the Wrubel Computing Center, and the taxpayers of the state of Indiana for support of this work. M.H.C. is also grateful for a Camille and Henry Dreyfus Teacher-Scholar Grant.

Registry No. $W_2(O\text{-}i\text{-}Pr)_6(py)_2$, 70178-75-5; $W_2(O\text{-}i\text{-}Pr)_6(py)_2(\mu\text{-}CO)$, 83436-99-1; $Mo_2(O\text{-}i\text{-}Pr)_6(py)_2(\mu\text{-}CO)$, 83437-00-7; $Mo_2(O\text{-}i\text{-}Pr)_6$, 62509-78-8; $W_2(ONeo)_6(HNMe_2)_2(m\text{-}CO)$, 83437-01-8; $W_2(ONeo)_6(HNMe_2)_2$, 83437-02-9; $Mo_2(ONeo)_6(HNMe_2)_2(\mu\text{-}CO)$, 83437-03-0; $Mo_2(ONeo)_6(HNMe_2)_2$, 83437-04-1; $Mo_2(ONeo)_6(py)_2(\mu\text{-}CO)$, 83437-05-2; $Mo_2(ONeo)_6(py)_2$, 81987-92-0; $Mo_2(O\text{-}i\text{-}Pr)_6(i\text{-}PrOH)_2(\mu\text{-}CO)$, 83447-51-2; $Mo_2(O\text{-}i\text{-}Pr)_6(\mu\text{-}CO)$, 83437-06-3; $Mo(CO)_6$, 13939-06-5; $Ti(O\text{-}i\text{-}Pr)_4$, 546-68-9.

Supplementary Material Available: Tables of observed and calculated structure factors and anisotropic thermal parameters (32 pages). Ordering information is given on any current masthead page. The complete structural reports, MSC Report No. 8062, $Mo_2(O\text{-}i\text{-}Pr)_6(py)_2(\mu\text{-}CO)$, and No. 81042, $W_2(O\text{-}i\text{-}Pr)_6(py)_2(\mu\text{-}CO)$, are available, in microfiche form only, from the Indiana University Chemistry Library.

Total Synthesis of Racemic Chorismic Acid and (−)-5-Enolpyruvylshikimic Acid ("Compound Z_1")

Donald A. McGowan and Glenn A. Berchtold*

Contribution from the Department of Chemistry, Massachusetts Institute of Technology, Cambridge, Massachusetts 02139.

Received April 14, 1982

Abstract: A new synthesis of methyl 4-*epi*-shikimate (**6**) is described. Ester **6** is used as the starting material for a total synthesis of racemic chorismic acid (**1**), the branch-point intermediate in the biosynthesis of aromatic amino acids and growth factors in microorganisms and higher plants. The procedure developed for the construction of the enolpyruvate functionality of **1** is applied also to the synthesis of (−)-5-enolpyruvylshikimic acid (**5**), a secondary metabolite derived from the biosynthetic precursor of chorismic acid.

The glucose-derived shikimate pathway and the acetate-derived polyketide pathway are the major routes for the biosynthesis of aromatic compounds from acyclic, nonaromatic precursors in bacteria, fungi, and higher plants. The shikimate pathway is better understood due to the successful isolation of discrete intermediates.[1] Chorismic acid (**1**, Scheme I) is the last common intermediate in aromatic biosynthesis from shikimic acid. Unambiguous proof that **1** is the intermediate between 5-enolpyruvylshikimic acid 3-phosphate (**2**) and prephenic acid (**3**) in the biosynthesis of phenylalanine and tyrosine was estabished after Gibson and collaborators developed a mutant of *A. aerogenes* from which **1** was isolated,[2] and the structure and absolute stereochemistry were determined.[3] Other work has established that **1** serves also as a biosynthetic precursor to *p*-aminobenzoic acid, anthranilic acid, tryptophan, hydroxybenzoic acids, and numerous other aromatic derivatives.[1] Of special interest from the chemical standpoint are the enzyme-catalyzed rearrangement of **1** to isochorismic acid (**4**)[4] and to **3**. The latter transformation, presumably a Claisen rearrangement, is unique to **1** and **4**, and in the case of **1**, the enzymatic reaction has been studied in detail.[5]

Scheme I

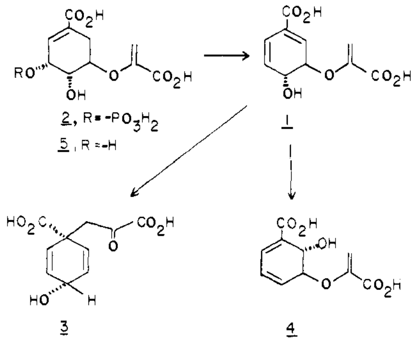

---

[1] (a) Weiss, U.; Edwards, J. M. "The Biosynthesis of Aromatic Compounds"; Wiley: New York, 1980. (b) Haslam, E. "The Shikimate Pathway"; Wiley: New York, 1974. (c) Ganem, B. *Tetrahedron* **1978**, *34*, 3353–3383.

[2] (a) Gibson, M. I.; Gibson, F. *Biochim. Biophys. Acta* **1962**, *65*, 160–163. (b) Gibson, F.; Jackman, L. M. *Nature* (*London*) **1963**, *198*, 388–389.

[3] Edwards, J. M.; Jackman, L. M. *Aust. J. Chem.* **1965**, *18*, 1227–1239.

[4] Young, I. G.; Batterham, T. J.; Gibson, F. *Biochim. Biophys. Acta* **1969**, *177*, 389–400; **1968**, *165*, 567–568.

0002-7863/82/1504-7036$01.25/0